

Imaging and monitoring with industrial seismic noise.

M. Campillo

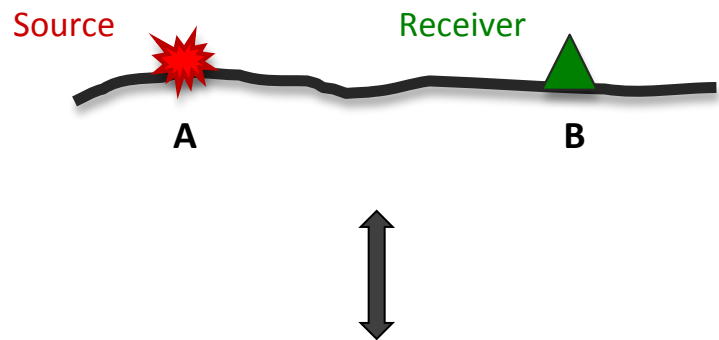


also :



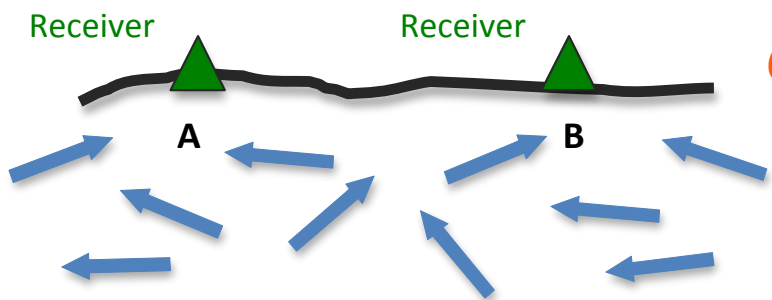
Boston, May 2016

Passive imaging: Long range correlations



Source in A \Rightarrow the signal recorded in B characterizes the propagation between A and B.

→ **Green function** between A and B: G_{AB}

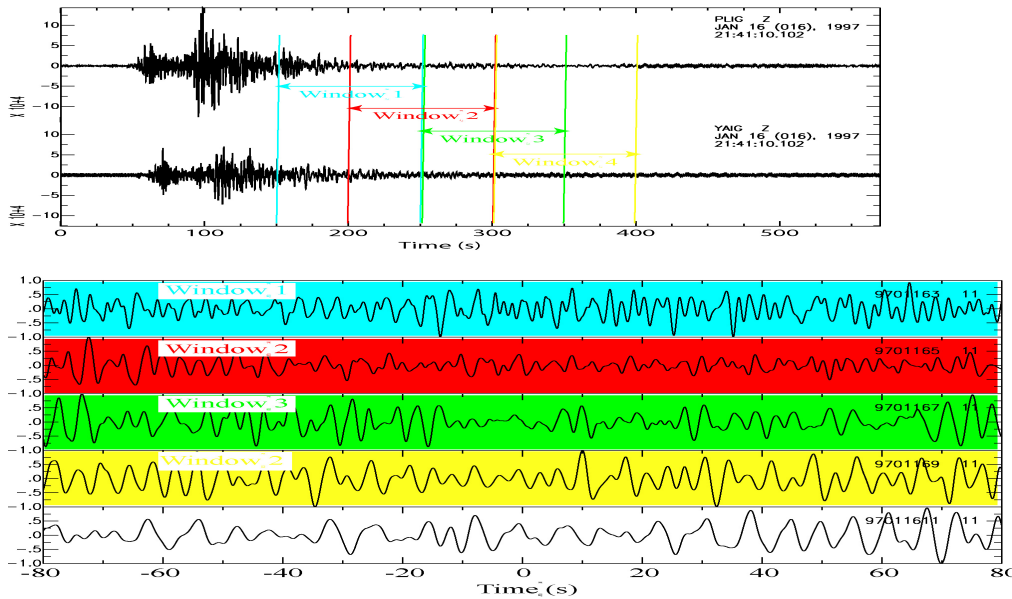


G_{AB} can be reconstructed by the correlation of noise or « diffuse » (equipartitioned) fields recorded at A and B (C_{AB})

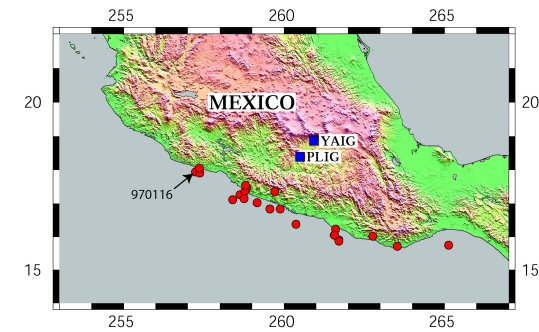
A way to provide new data with control on source location and origin time

Seismological application: coda waves

Individual cross-correlations: fluctuations dominate.



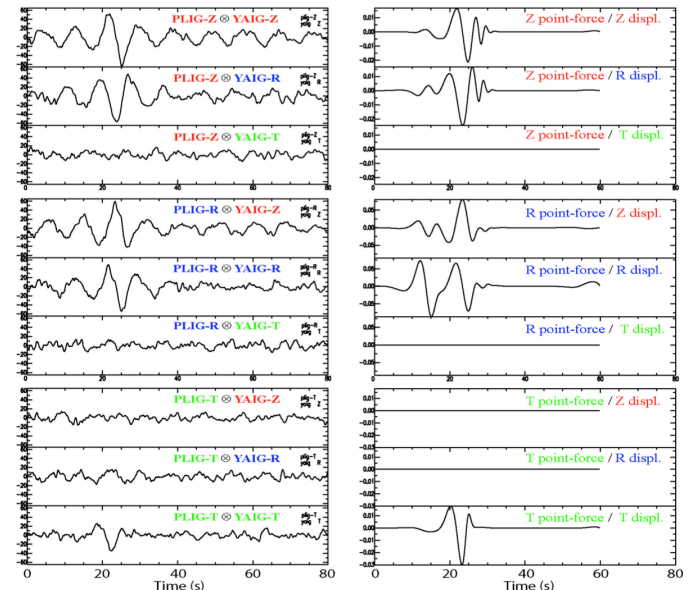
After averaging over 100 EQs →



Emergence of the Green function

Stacks of 196 cross-correlations

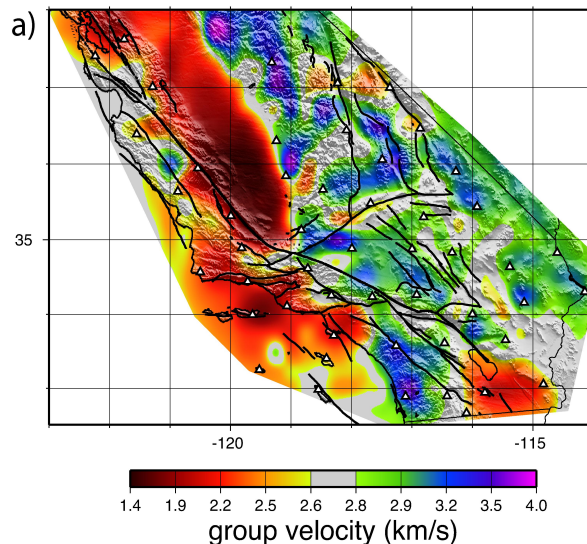
Theoretical Green tensor at 69 km distance



Cross-correlations of coda and noise records ≈ Green functions = virtual seismograms

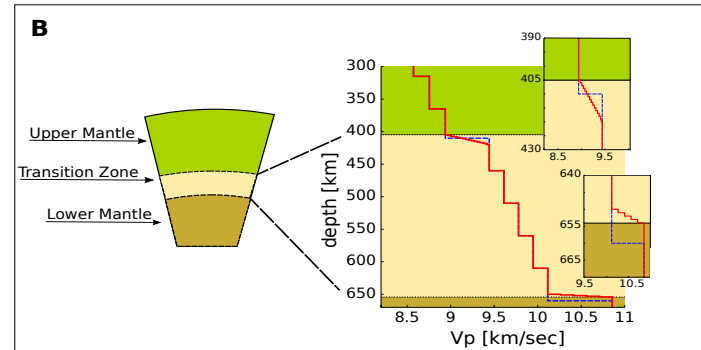
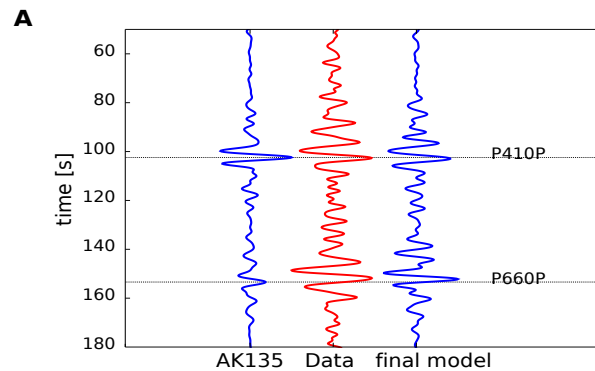
-demonstrated for the retrieval of surface waves (e.g. Paul and Campillo, 2001; Campillo and Paul, 2003; Shapiro and Campillo, 2004....) or body waves (e.g. Zhan et al., 2010 ; Poli et al., 2012).

High resolution velocity map of California obtained from ambient noise (Rayleigh)
(Shapiro, Campillo, Stehly and Ritzwoller, Science 2005)



Large N sensor array \Rightarrow $N^2/2$ correlations

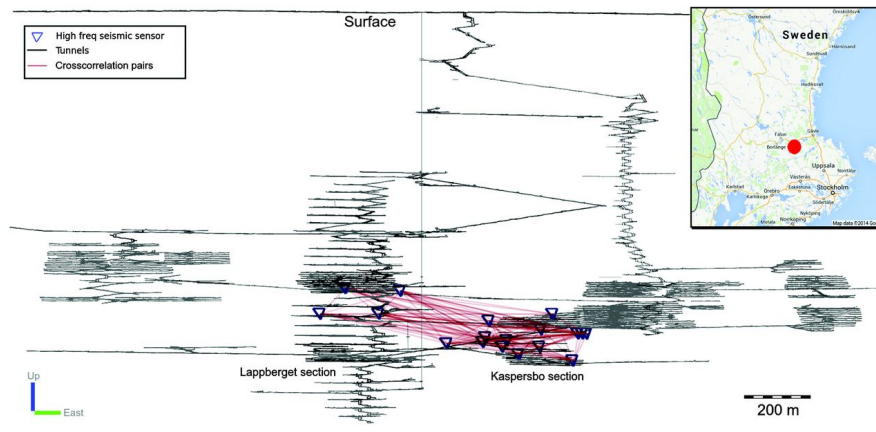
**Earth's mantle discontinuities from ambient noise
(phase transition \rightarrow (P, T))**
Body waves (Poli et al., 2012)
Poli, Campillo, Pedersen. Science 2012



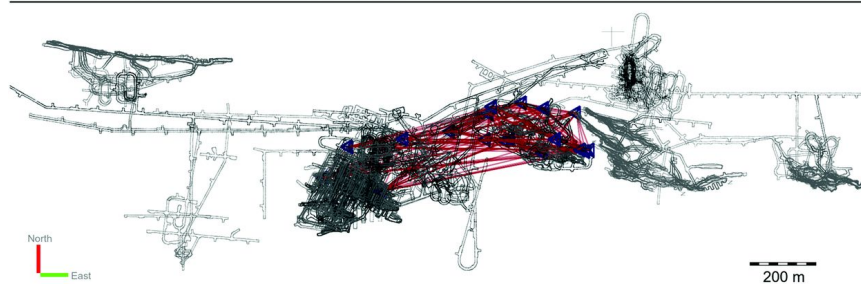
Smaller scale, industrial environment

Active mine: various sources of noise
tunnels (scattering)

Section view

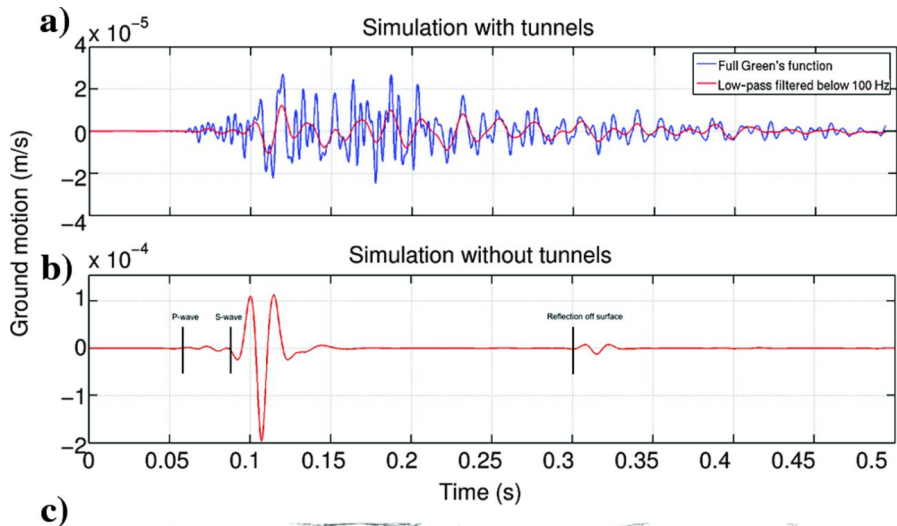


Plan view

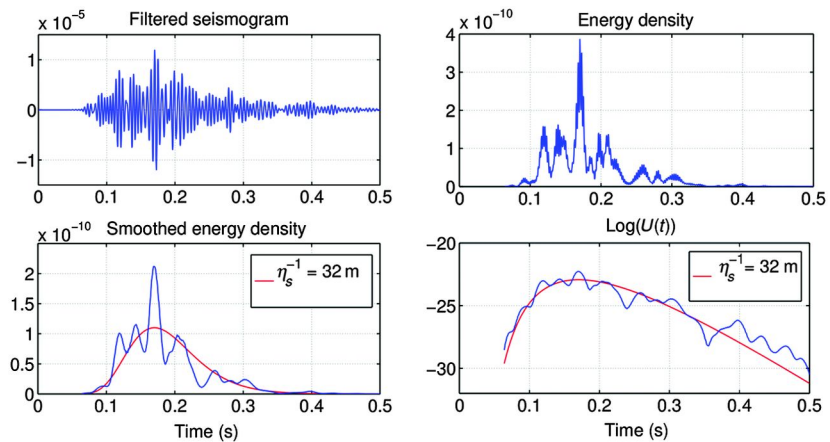


Results from Olivier, Brenguier, Campillo, Lynch and Roux, 2015
GEOPHYSICS, VOL. 80, NO. 3 (MAY-JUNE 2015); P. KS11-KS25

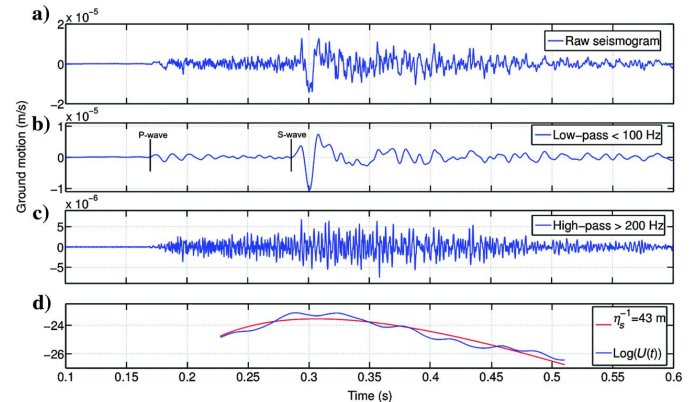
Numerical simulation in presence of the tunnels



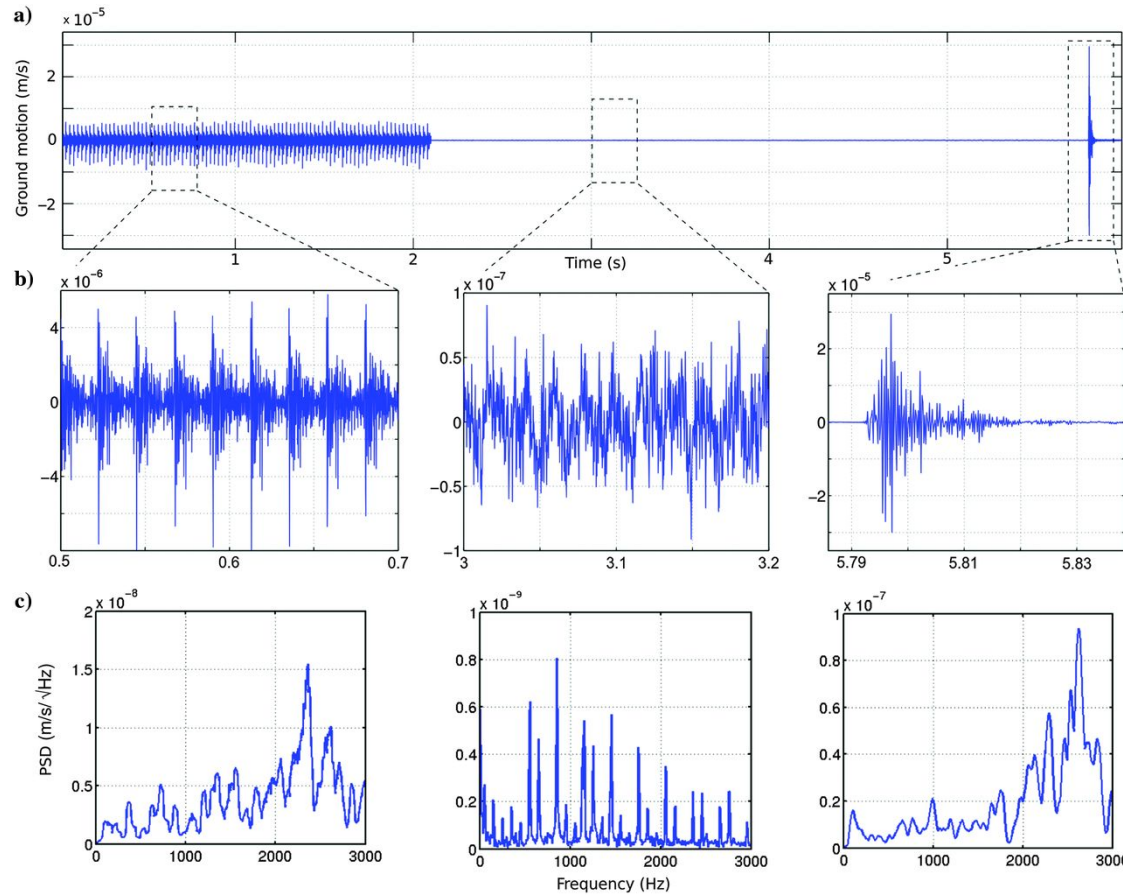
Synthetics vs Diffusion approximation



Actual event vs Diffusion approximation



Nature of the noise: example of a 5s record

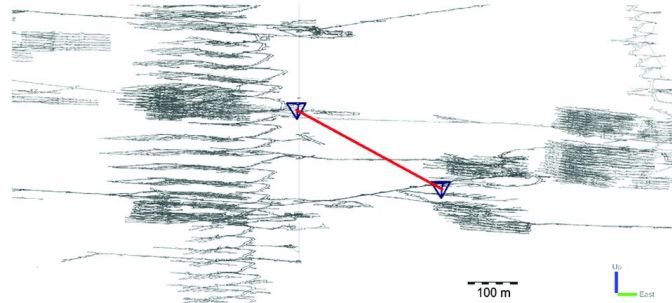
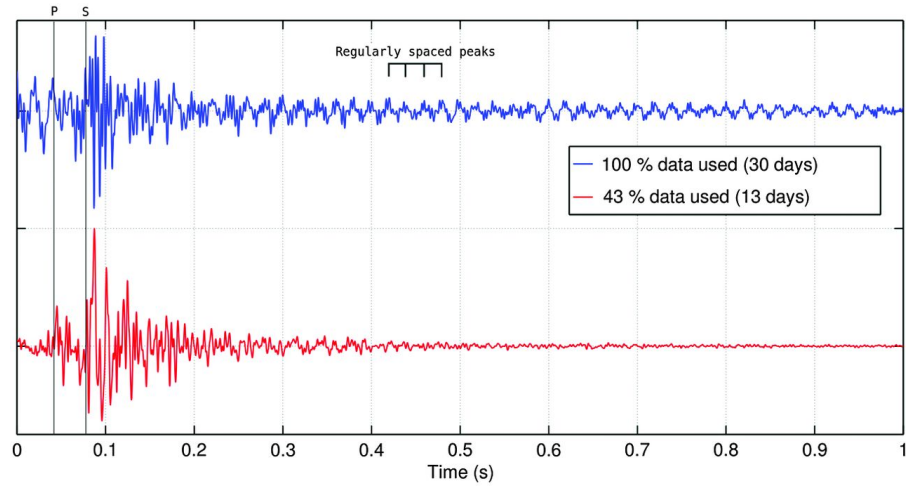


impacts of a hammer drill

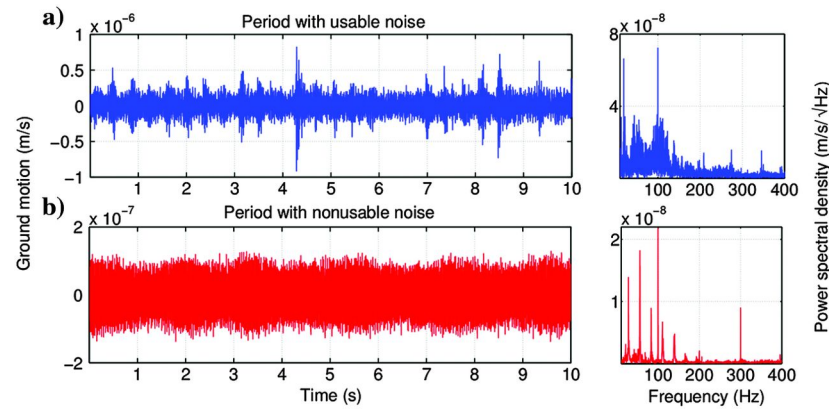
microseismic event

multiple sources
incl. (pumps, fans, etc.)

Correlation functions (ZZ)



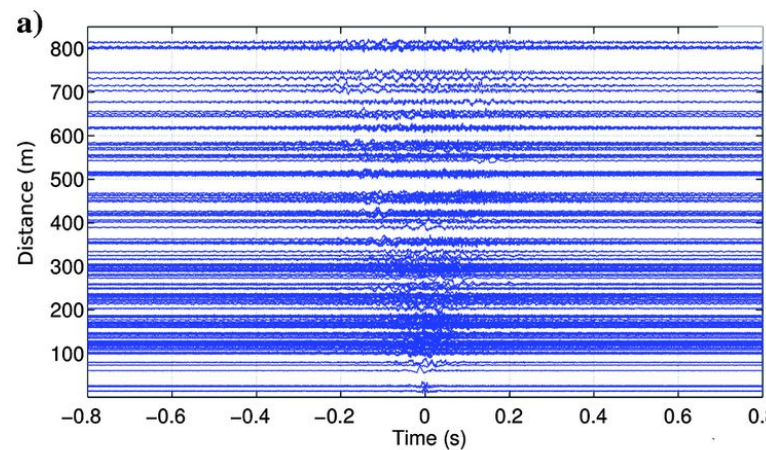
Selective stacking: optimal time windows for body wave contributions:



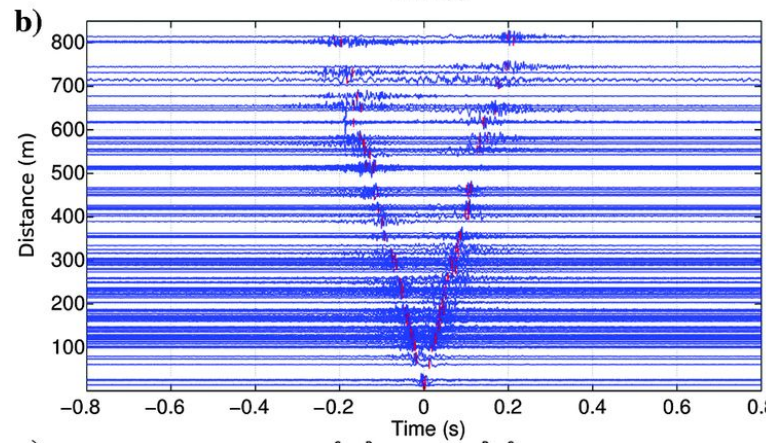
Removing of monochromatic sources

ZZ time-distance sections

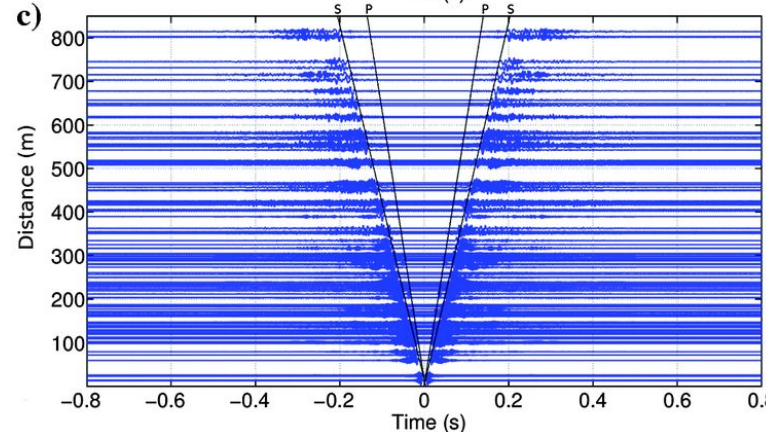
Noise correlations: blind stacking



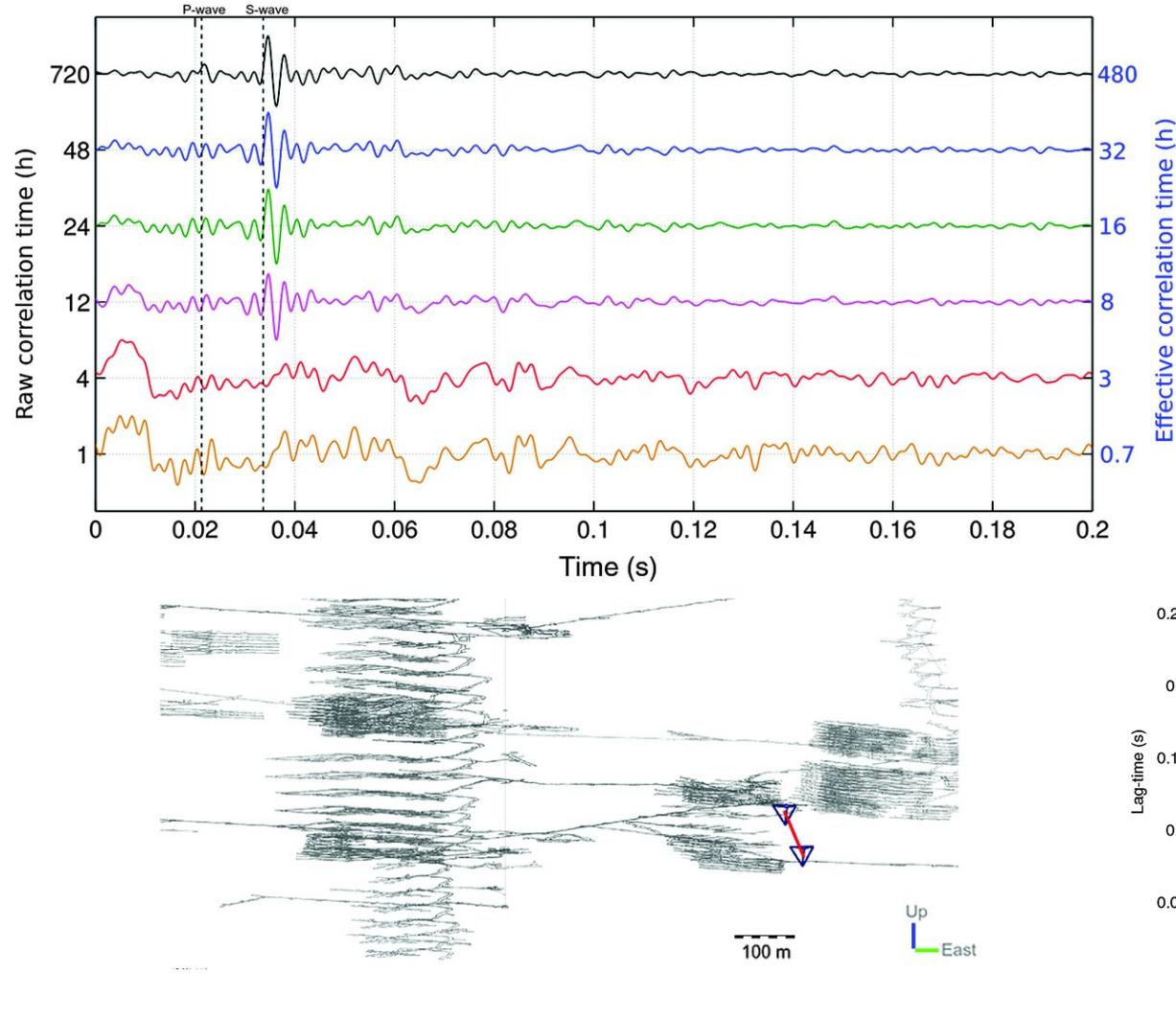
Noise correlations: optimal stacking



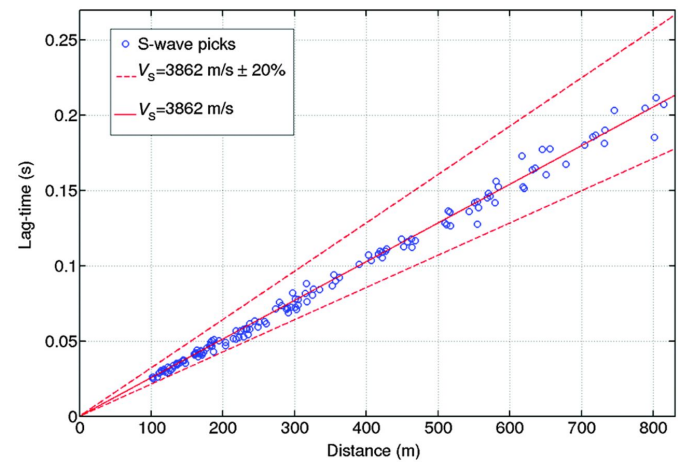
Synthetics



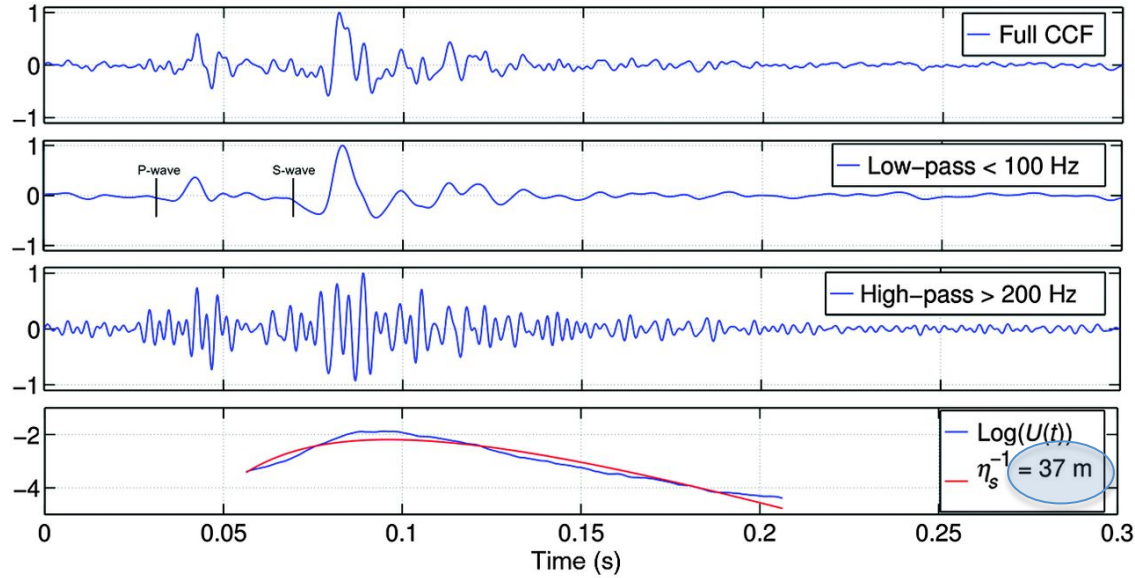
Convergence of the ZZ correlation function



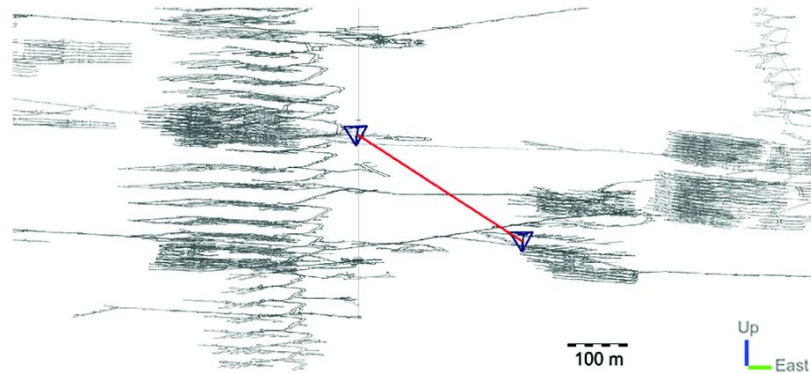
S wave velocity



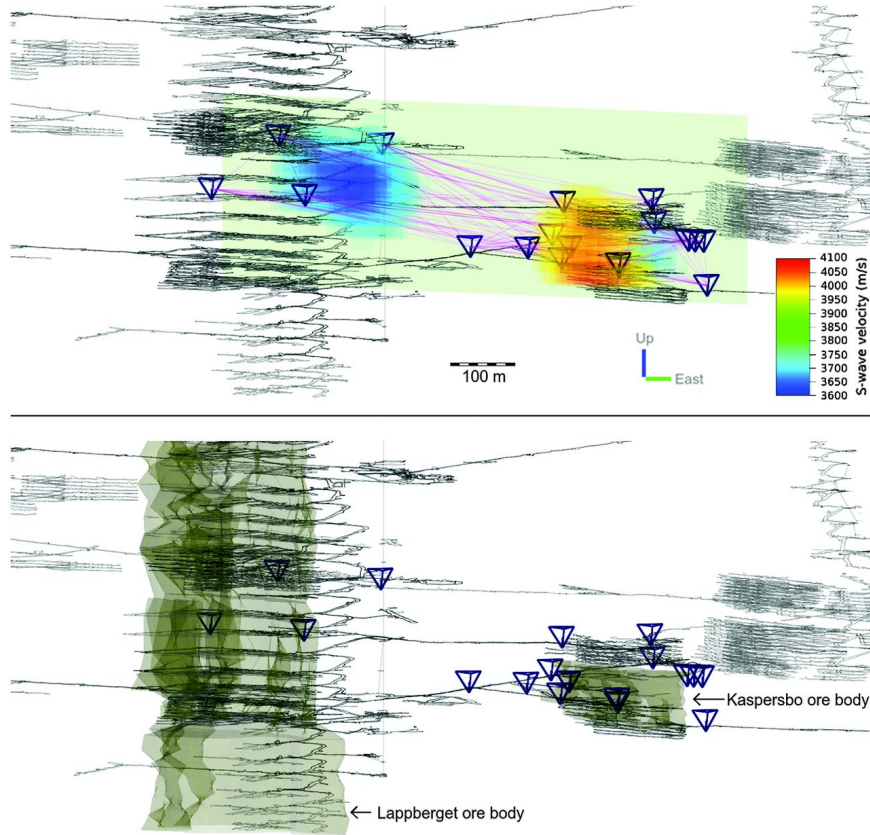
Scattering properties from noise correlations



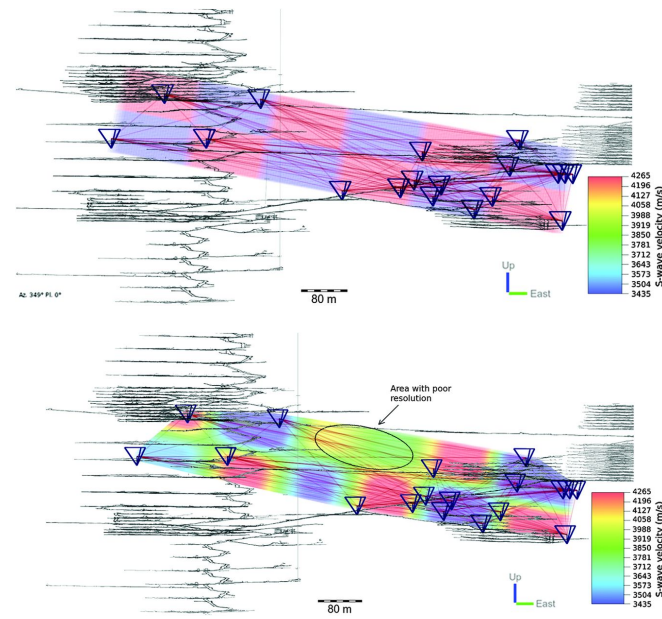
Diffusion approx.



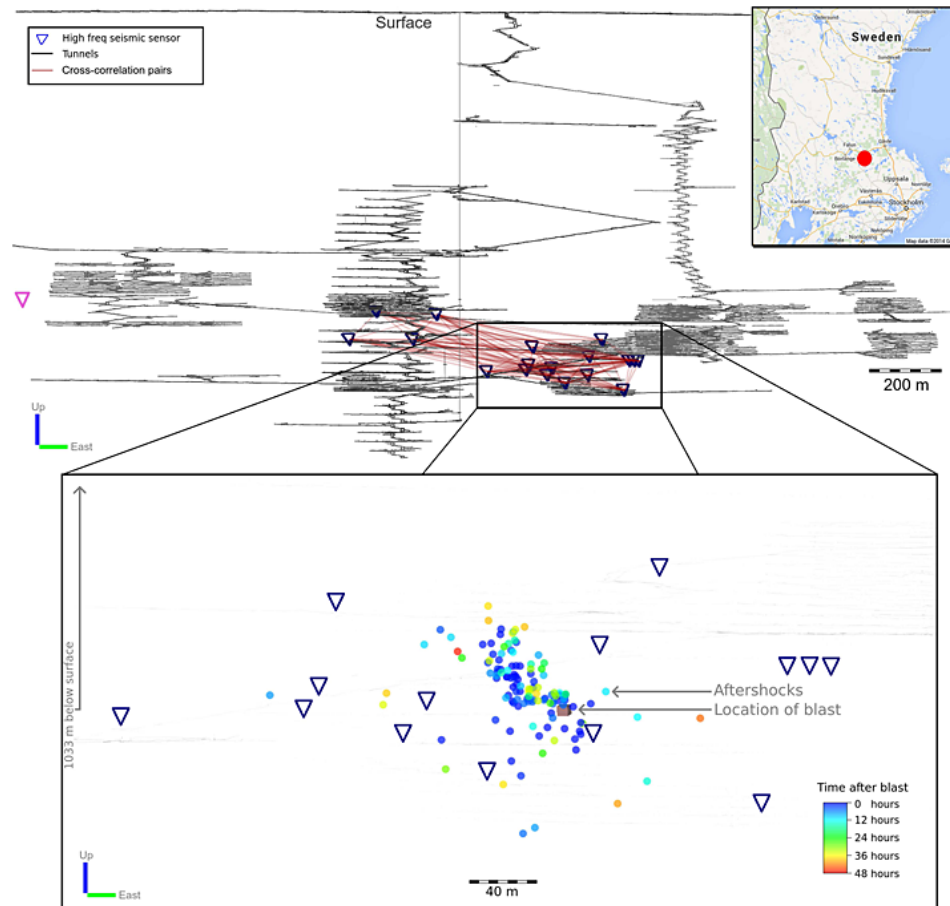
Travel time tomography from noise correlations



Checkboard test

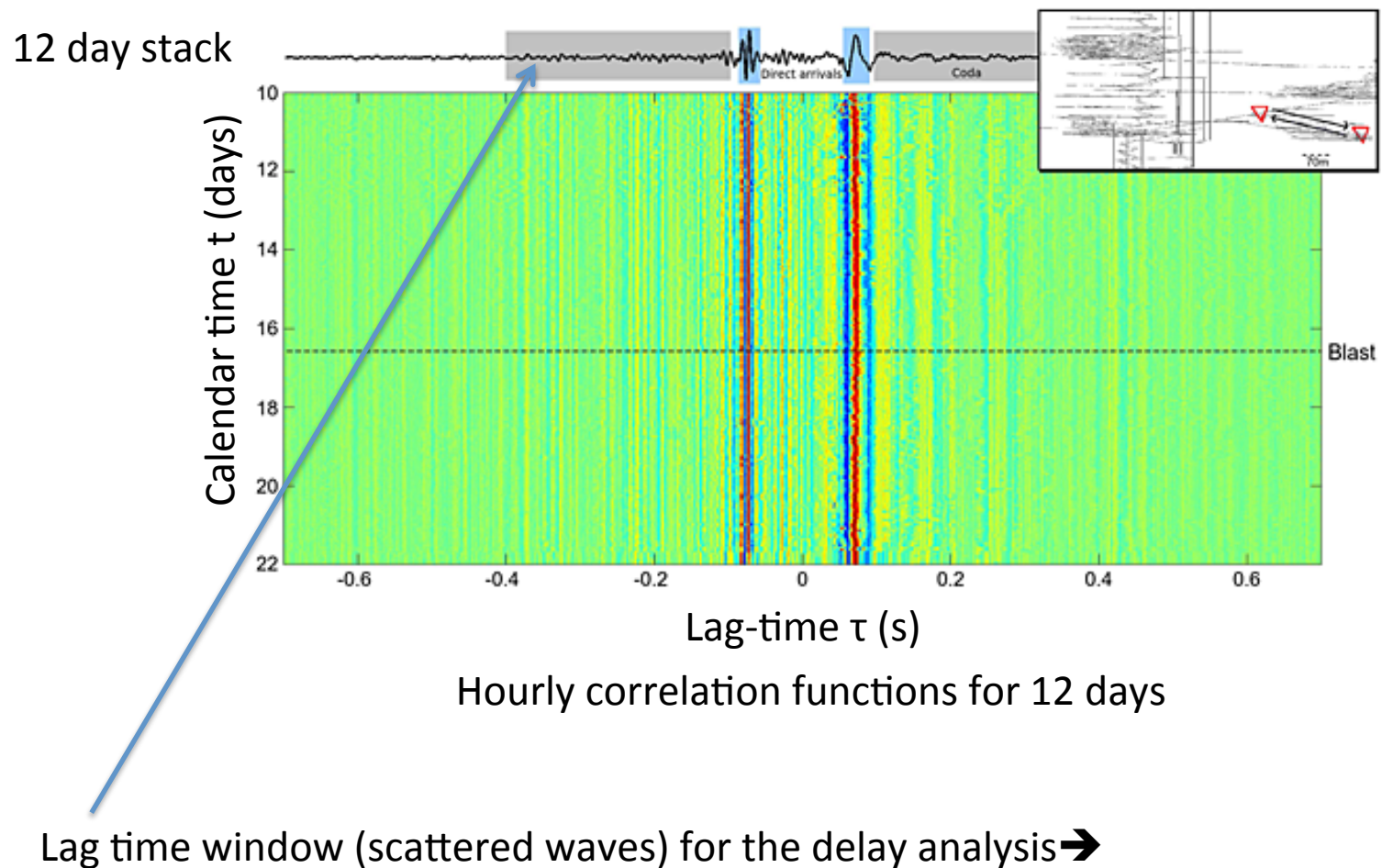


Investigation of coseismic and postseismic processes using in situ measurements of seismic velocity variations in an underground mine



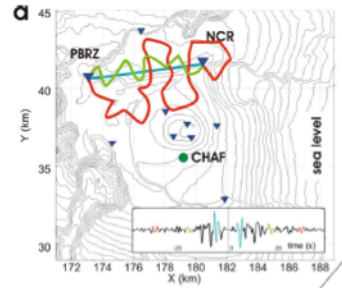
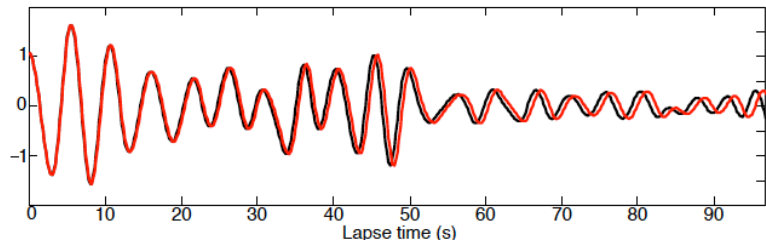
Results from Olivier, Brenguier, Campillo, Roux, Shapiro and Lynch, 2015 **Geophysical Research Letters**
[Volume 42, Issue 21](#), pages 9261-9269, 11 NOV 2015 DOI: 10.1002/2015GL065975
<http://onlinelibrary.wiley.com/doi/10.1002/2015GL065975/full#grl53668-fig-0001>

Investigation of coseismic and postseismic processes using in situ measurements of seismic velocity variations in an underground mine

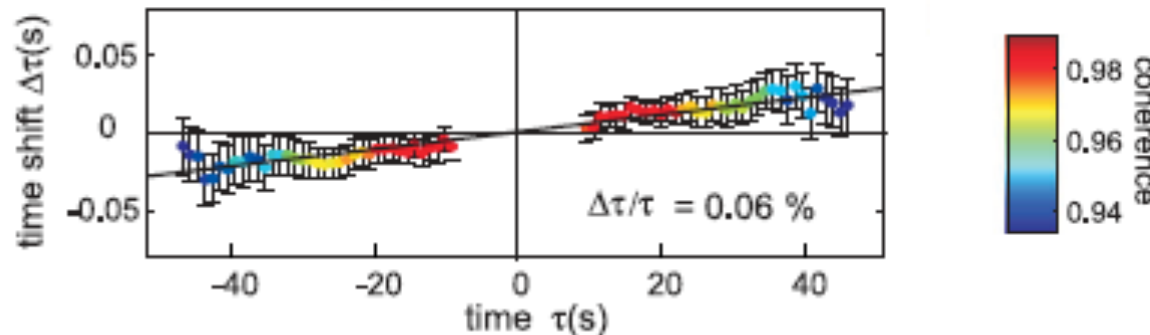


Detecting a small change of seismic speed: coda waves

Comparing a trace with a reference under the assumption of an homogeneous change



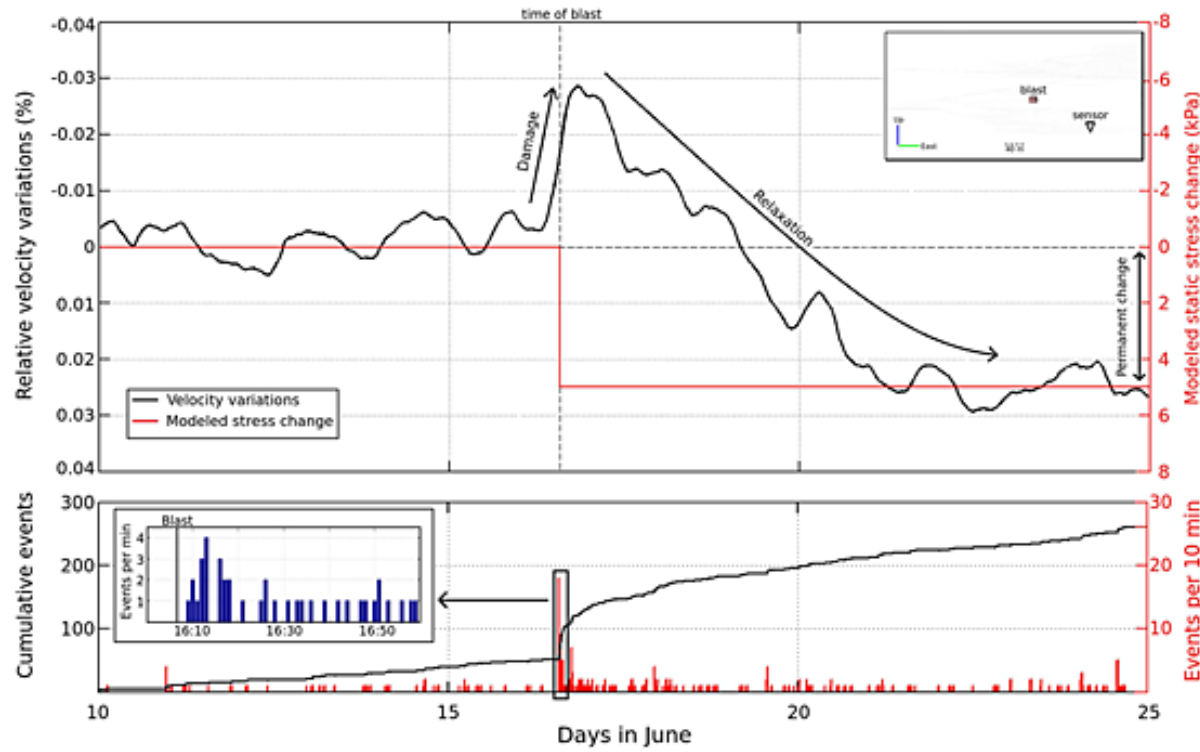
The ‘doublet’ method: moving window cross spectral analysis of the delays



Relative velocity change:

$$\frac{dV}{V}(t) = -\frac{d\tau}{\tau}(t)$$

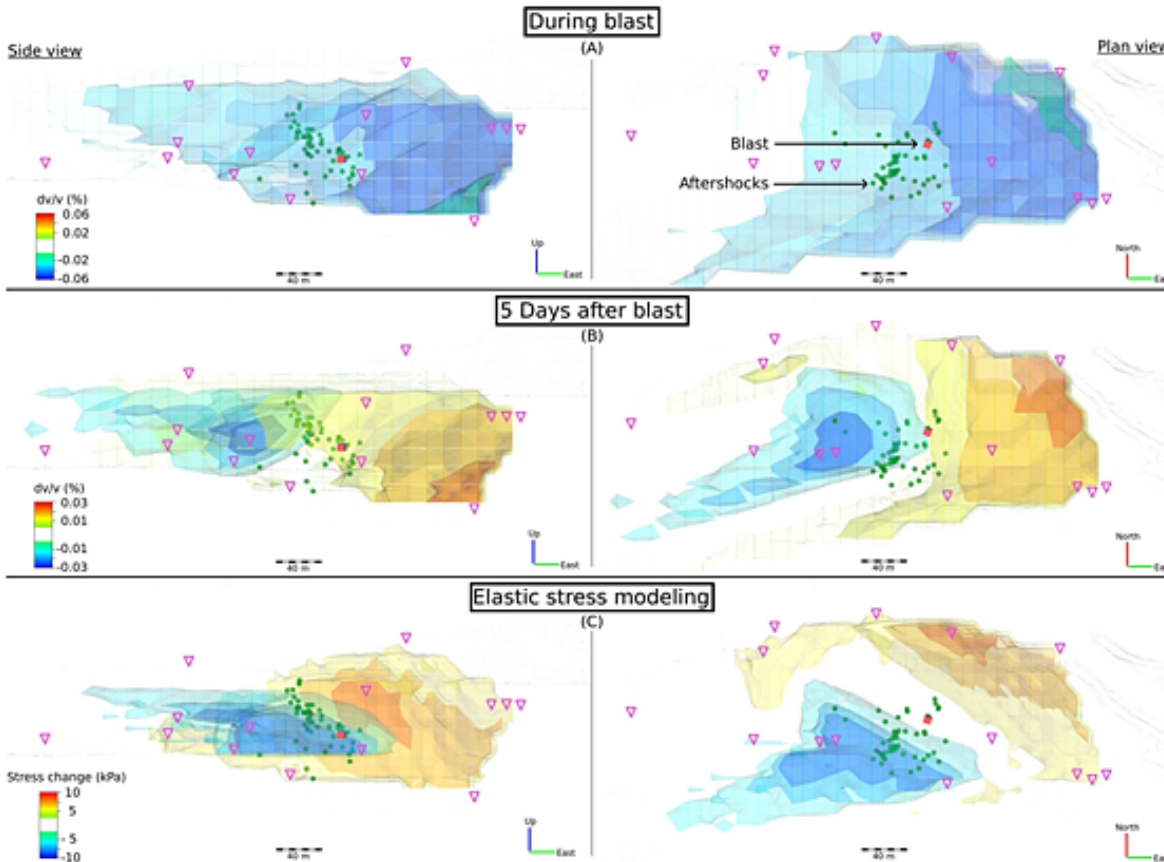
Temporal evolution of the seismic velocity measured from all correlations involving a particular sensor (4 hour window)



The relaxation time is larger than the one deduced from detected seismicity

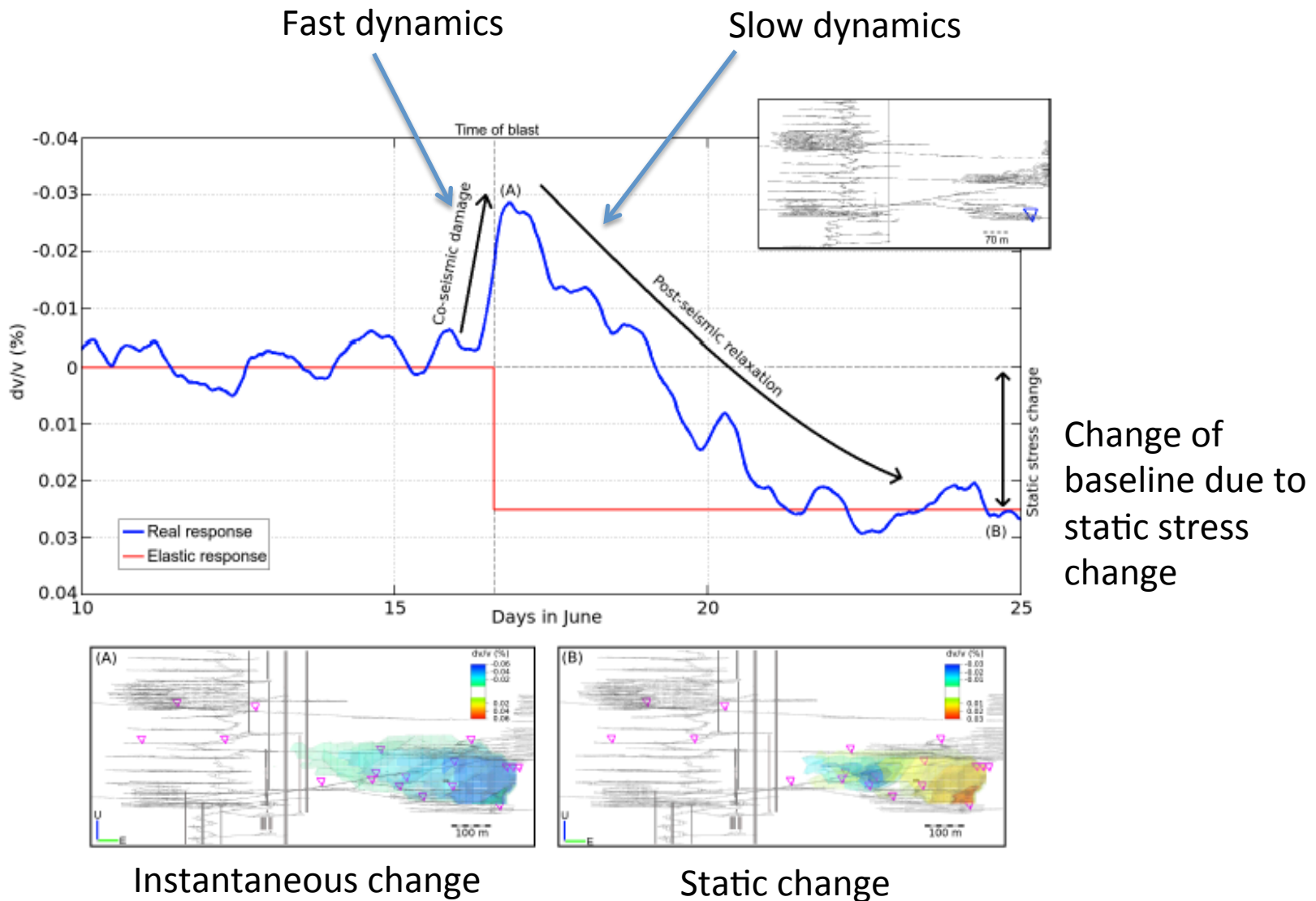
Comparison of velocity changes and volumetric stress changes

Instantaneous velocity drop



'Static' change

Velocity change due to blast and excavation



Conclusions:

Passive (noise based) imaging is possible in industrial environment like mines.

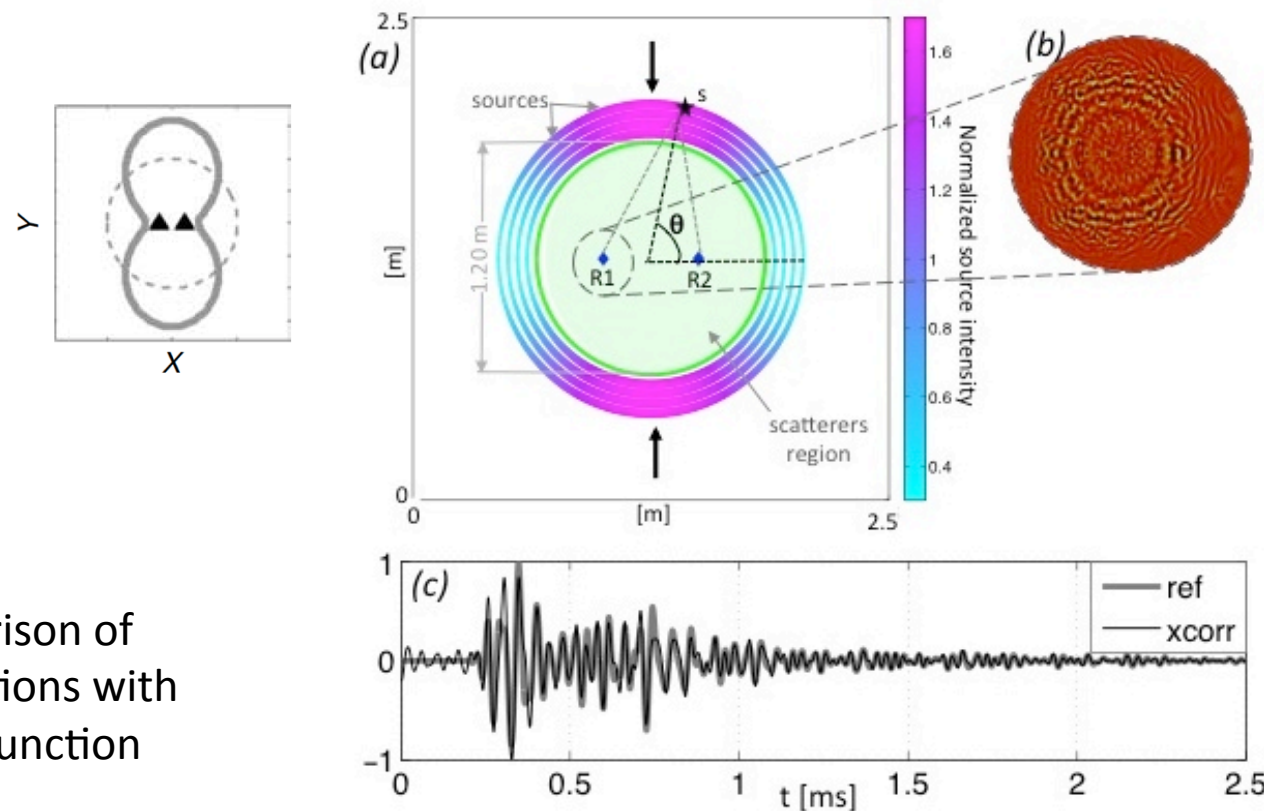
It requires a careful analysis of the noise properties

Body waves are retrieved and could be used for imaging

Time dependent elastic properties can be inferred giving new clues on the geomechanical evolution

Measuring slight changes of seismic velocity using coda waves (long travel time) Numerical simulations in a scattering medium

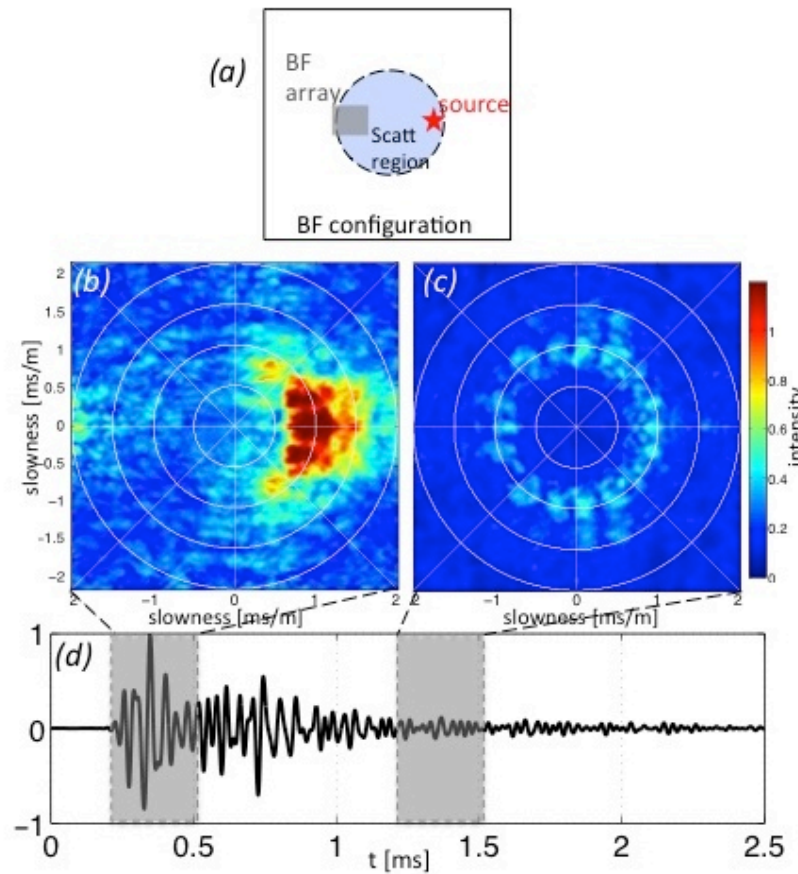
2D spectral elements, anisotropic intensity of sources



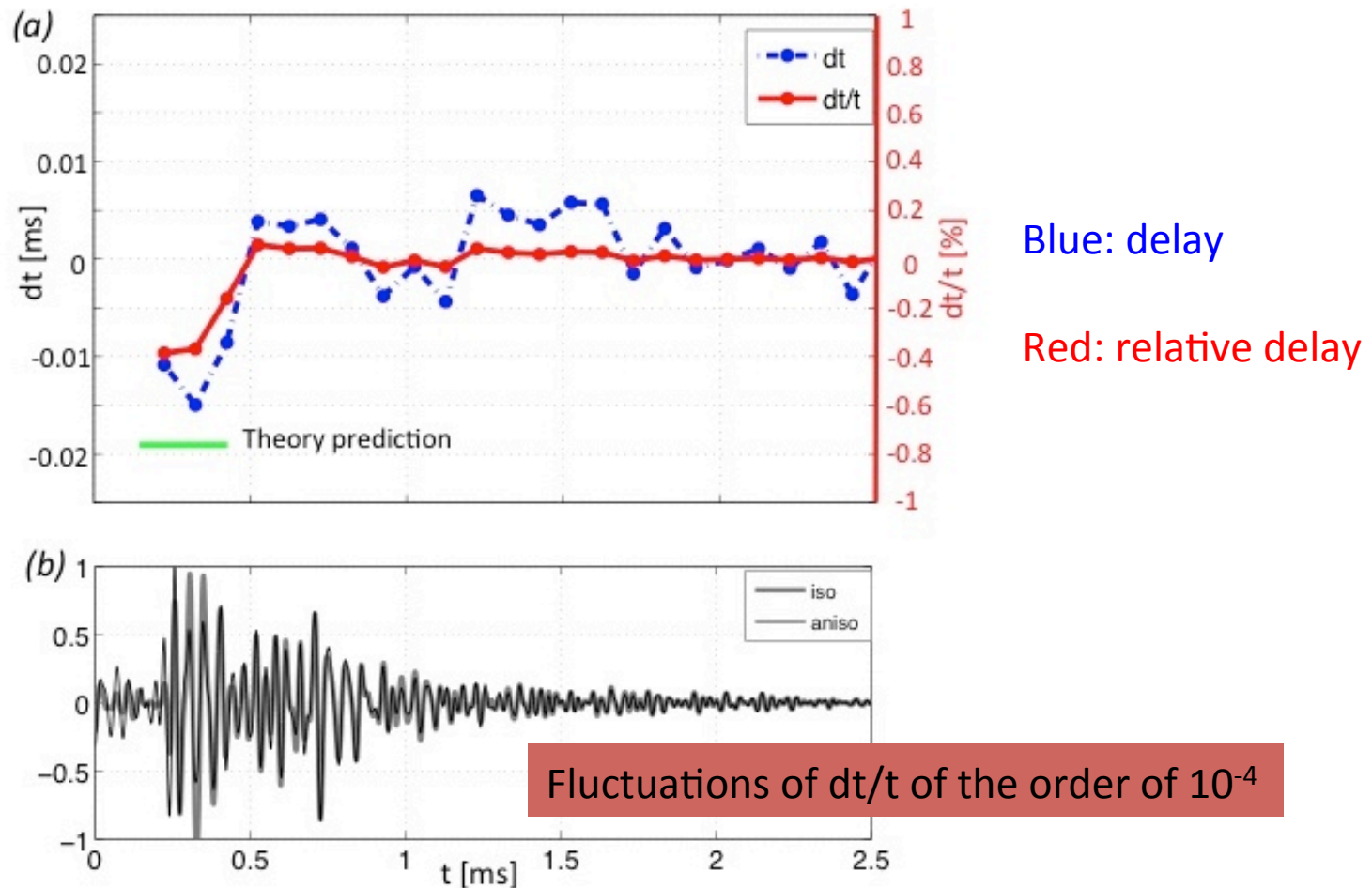
Comparison of correlations with Green function

Effect of scattering (single source)

Beam forming

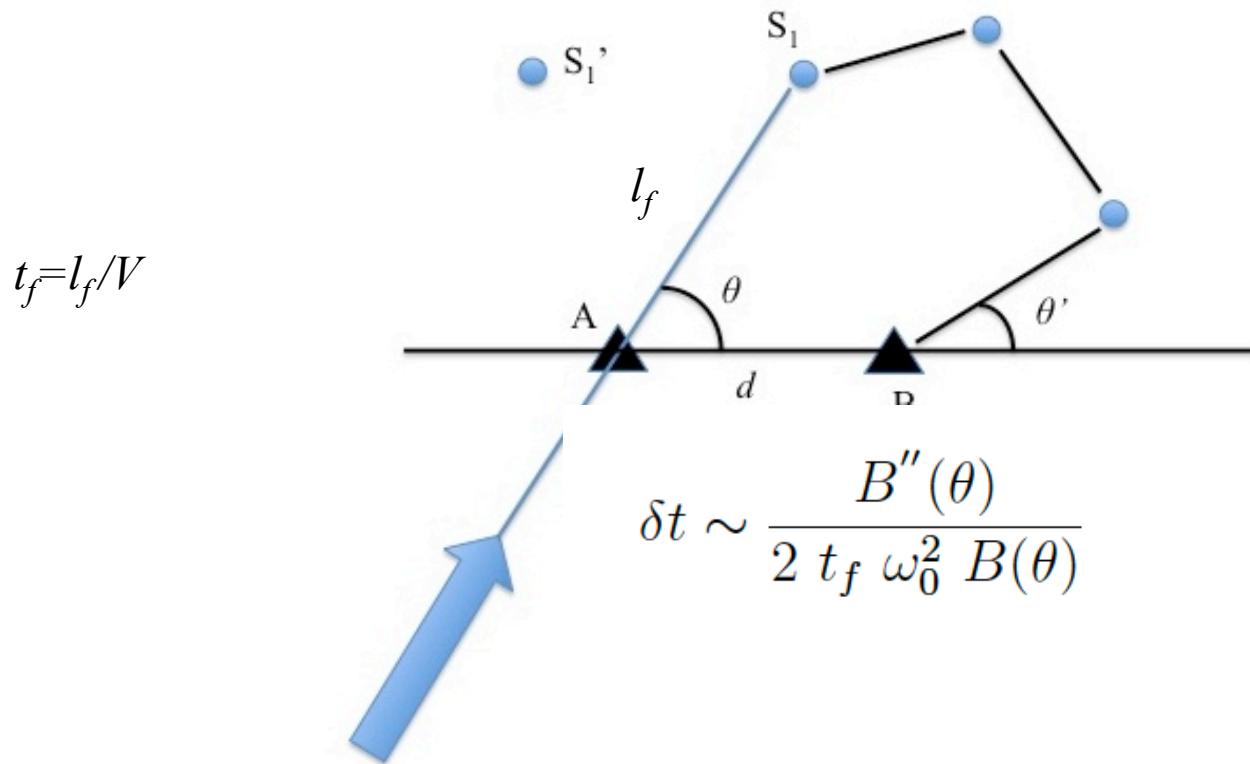


Measure of the bias induced by a strong anisotropy of the wave field (delay with respect to the Green function)



Representation of coda waves as the sum of contributions of numerous paths

For a single path:



We have to compute the contributions of paths with first scatterers at all distances l_f and all azimuths θ

We have to consider that the distribution of distance between scattering events is exponential:

$$P(l_f) = \frac{1}{l} e^{-\frac{l_f}{l}} \quad \text{where } l \text{ is the mean free path} \quad \langle l_f \rangle = l \quad t_f = l_f / V$$

We make use of

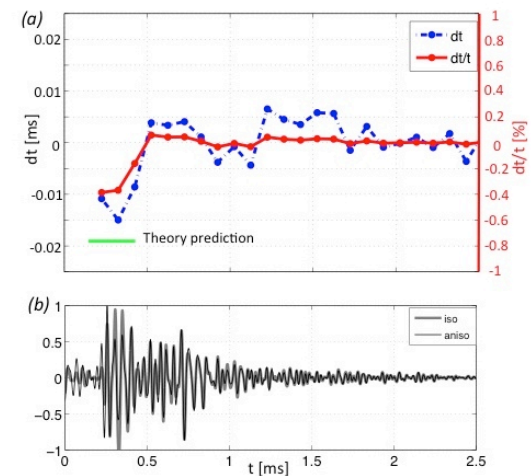
$$\delta t \sim \frac{B''(\theta)}{2 t_f \omega_0^2 B(\theta)} \quad \text{valid for } l_f > \lambda$$

Applications

Numerical simulations

$l = 0.5m$, $c = 2000\text{m/s}$,

$f_0 = 30000\text{Hz}$, $B_2 = -0.6$ and $\tau_m = 0.002\text{s}$



→ fractional error $\frac{\delta t(\tau_m)}{\tau_m}$ of 10^{-4}

